SPE 36856

Capillary Trapping in Three-Phase Flow

G.A. Virnovsky, SPE, Rogaland Research, S.M. Skjaeveland, SPE, Stavanger College, H.M. Helset, SPE, Rogaland Research

This paper was prepared for presentation at the 1996 SPE European Petroleum Conference held in Milan, Italy, 22-24 October 1996.

Abstract

The paper presents the results of analytical and numerical studies of the capillary trapping phenomena occurring in 3-phase flow. Based on theoretical results, a numerical procedure and a software package has been developed providing an easy way to compute distribution of residual oil in a heterogeneous 1D reservoir.

For a given set of relative permeabilities and capillary pressure, the saturation profiles are generated for different types of wettability of the rock and different types of boundary conditions which are relevant for reservoir and laboratory. The main characteristics influencing the process of capillary trapping are wettability type, and the 2 capillary numbers showing the relative strength of capillary forces for oil-water and oil-gas as compared to the viscous forces. It is shown that the type of boundary conditions as well as wettability will strongly influence the amount of the capillary trapped oil and gas.

Introduction

Capillary trapping due to the reservoir heterogeneity plays an important role in many oil recovery processes where multiphase flow is encountered. In the present paper we are not considering the trapping phenomena occurring on the pore scale. The dispersed phases saturation (i.e. relative permeability is zero) which can not be reduced without reduction of interfacial tension is therefore not addressed. The subject of the paper is the capillary trapping effects due to heterogeneity of medium scale. Taking place on the scale of order of centimeters to meters these effects can not be explicitly simulated in a full-field scale study, but are rather represented indirectly, i.e., through the so called upscaled relative permeabilities.

Capillary effects in two-phase steady-state flow have previously been analyzed in a number of papers [8, 3, 6]. To the best of our knowledge this is the first paper addressing the issue in case of three-phase flow. The system of equations describing the steady-state three-phase flow is similar to the previously considered system describing stable movement of displacement fronts in case of three-phase gravity segregated flow[7] and is analysed in a similar manner.

The importance of considering three-phase flow is dictated from practical needs. It makes it possible to consider the influence of free gas on residual oil and therefore to evaluate WAG or depressurization as compared to water flooding. Another field of application is interpretation of the three-phase core flooding experiments with account for capillary effects. Since the classical paper[5] it is recognized that capillary forces significantly affect laboratory experiments though neglected in a standard interpretation procedure. In order to plan the experiments, and also to properly understand and interpret the results the considered steady-state three-phase model may be utilized.

Steady-state three-phase flow

Three-phase steady state model is formulated as an extension of a similar two-phase one described in Refs. 8 and 3.

The system of equations describing three-phase flow under the assumptions that compressibility and solubility of phases is neglected consists of a conservation law and the Darcy's law for each of the phases, two capillary pressure relationships, and a trivial relationship for the saturations:

$$\phi \frac{\partial S_i}{\partial t} + \frac{\partial u_i}{\partial x} = 0, \qquad i = 1, 2, 3 \quad .... (1)$$

$$u_i = -\kappa(x) \frac{k_{ri}(S_1, S_3)}{\mu_i} \left(\frac{\partial p_i}{\partial x} - \rho_i g_x \right),$$

$$p_2 - p_1 = \pi_1(S_1, \kappa), \quad p_3 - p_2 = \pi_3(S_3, \kappa),$$
$$\sum_{i=1}^{3} S_i = 1.$$

We assume for convenience that the phases are numbered with respect to wettability, so that index 1 corresponds to the most wetting phase (e.g., water), index 3 corresponds to the most non-wetting phase (gas), while index 2 is left for the intermediate wetting phase (oil).

Note that in the above formulation (1) the capillary pressures are assumed to be functions of only one argument. This type of representation of three-phase capillary pressures is described in Ref. 1, and is implemented in some commercial simulators, e.g., *ECLIPSE*. Though this is justified by some experimental evidence, Ref. 4, the reason for the usage of this formulation in simulations is, probably, of purely utilitarian nature: a set of 2 two-phase capillary pressure curves constitutes the minimal amount of data required to simulate three-phase flow which can be reliably obtained from standard laboratory experiments. To the best of our knowledge, there exists no standard procedure to determine three-phase capillary pressure functions (as functions of 2 arguments).

The phase pressures may be eliminated from Eqs. (1) in a standard way giving a closed system of two equations for two unknown saturations.

$$\phi \frac{\partial \mathbf{S}}{\partial t} + U \frac{\partial \mathbf{F}}{\partial x} = \frac{\partial}{\partial x}(\kappa(x) A \frac{\partial \pi}{\partial x}) \quad \text{..............(2)}$$

$$\frac{\partial U}{\partial X} = 0, \quad U = \sum_{i=1}^{3} u_i,$$

$$F_i = \frac{\lambda_i}{\sum_{j=1}^{3} \lambda_j}(1 + \frac{\kappa}{U} g_x \sum_{j \neq i}^{3} \lambda_j \Delta\rho_{ij}),$$

$$\Delta\rho_{ij} = \rho_i - \rho_j, \quad \lambda_i = f_i / \mu_i, \quad i = 1,2$$

$$\pi = \begin{pmatrix} \pi_1 \\ \pi_3 \end{pmatrix}, \quad \mathbf{F} = \begin{pmatrix} F_1 \\ F_3 \end{pmatrix}, \quad \mathbf{S} = \begin{pmatrix} S_1 \\ S_3 \end{pmatrix}$$

$$A = \begin{pmatrix} -\frac{\lambda_1}{\lambda_t}(\lambda_2 + \lambda_3) & -\frac{\lambda_1}{\lambda_t}\lambda_3 \\ \frac{\lambda_3}{\lambda_t}\lambda_1 & \frac{\lambda_3}{\lambda_t}(\lambda_1 + \lambda_2) \end{pmatrix}$$

A steady state three-phase flow is therefore governed by the system of equations

$$U \frac{d\mathbf{F}}{dx} = \frac{d}{dx}(\kappa(x) A \frac{d\pi}{dx}) \quad \text{..............(3)}$$

By integration one obtains

$$U(\mathbf{F}(\mathbf{S}) - \mathbf{F}^0) = \kappa A(\mathbf{S}) \frac{d\pi}{dx}, \quad \text{..............(4)}$$

$$\mathbf{F}^0 = \begin{bmatrix} F_1^0 \\ F_3^0 \end{bmatrix}, \quad F_i^0 = u_i / U.$$

Since

$$\det A = -\frac{\lambda_1 \lambda_2 \lambda_3}{\lambda_t}$$

det A is non-positive. It is zero on the boundaries of the triangle Δ_s defined by

$$\Delta_s = \{S_1, S_3 | S_1 \geq 0, S_3 \geq 0, S_1 + S_3 \leq 1\} \quad \text{..............(5)}$$

where phase mobilities are zero.

If the capillarity matrix A has a non-zero determinant an inverse matrix exists:

$$A^{-1} = \frac{1}{\det A} \begin{pmatrix} \frac{\lambda_3}{\lambda_t}(\lambda_1 + \lambda_2) & \frac{\lambda_1}{\lambda_t}\lambda_3 \\ -\frac{\lambda_3}{\lambda_t}\lambda_1 & -\frac{\lambda_1}{\lambda_t}(\lambda_2 + \lambda_3) \end{pmatrix} \quad \text{.. (6)}$$

In case when the inverse matrix exists Eq. (4) may be rewritten as

$$\frac{d\pi}{dx} = \frac{U}{\kappa} A^{-1}(\mathbf{F}(\mathbf{S}) - \mathbf{F}^0) \quad \text{..............(7)}$$

After substitution of Eq. (6) into Eq. (7) and some algebraic manipulations one obtains the following system of two ordinary differential equations describing steady state saturations distribution along the coordinate:

$$\frac{d\pi_1}{dx}=-\frac{U}{\kappa}\left[\frac{F_2^0}{\lambda_2}-\frac{F_1^0}{\lambda_1}+\frac{\kappa}{U}g_x\Delta\rho_{12}\right]$$
$$\frac{d\pi_3}{dx}=\frac{U}{\kappa}\left[\frac{F_2^0}{\lambda_2}-\frac{F_3^0}{\lambda_3}+\frac{\kappa}{U}g_x\Delta\rho_{32}\right] \qquad (8)$$

Steady-state flow in homogeneous medium. As on can see from Eq. (4) the viscous limit point $\mathbf{S}^0$ defined by the system of equations $\mathbf{F}(\mathbf{S}^0)=\mathbf{F}^0$ is the rest point of the system of differential equations. We now analyze the behavior of the solutions in the vicinity of the rest point assuming homogeneous medium, and absence of gravity in the flow direction. In this case the capillary pressures are only functions of saturations, and the linearized system can be written as follows:

$$\frac{d\mathbf{S}}{dx}=\frac{U}{\kappa\lambda_t^0}R(\mathbf{S}^0)(\mathbf{S}-\mathbf{S}^0) \qquad (9)$$

The behavior of the system (9) depends on the eigenvalues of the matrix R. It can be shown that the matrix R has 2 real eigenvalues if the relative permeabilities of the 1-st and the 3-rd phases only depend on their own saturations, and the relative permeability of the 2-nd phase satisfies the condition

$$\frac{\partial k_{r2}}{\partial S_1}\frac{\partial k_{r2}}{\partial S_3}\geq 0 \qquad (10)$$

According to the standard classification the rest point in this case is always a node [2]. The node is non-attractive if the total velocity is positive. From this follows an important conclusion: to have a unique and stable solution the boundary conditions should be specified at the down-stream boundary.

Heterogeneous medium. In order to proceed, it is necessary to concretize the form of the capillary pressures dependence on their arguments. We therefore assume a Leverett-type relationship for the two capillary pressure functions:

$$\pi_i=\frac{\gamma_i}{\sqrt{\kappa}}J_i(S_i),\qquad \gamma_i=\sigma_i\sqrt{\phi} \qquad (11)$$

In the Eq. (11) we neglect variations of the porosity because of much more stronger variations of the absolute permeability normally encountered in oil reservoirs, e.g., 50% compared to tens of times. Then the dimensionless form of the system (8) reads

$$J_1'\frac{dS_1}{dX}=-\varepsilon_1\left[\frac{F_2^0}{k_{r2}}-\frac{F_1^0}{k_{r1}}M_1\right]-N_{g1}+J_1\frac{1}{\tau}\frac{d\tau}{dX}$$
$$J_3'\frac{dS_3}{dX}=\varepsilon_3\left[\frac{F_2^0}{k_{r2}}-\frac{F_3^0}{k_{r3}}M_3\right]+N_{g3}+J_3\frac{1}{\tau}\frac{d\tau}{dX} \qquad (12)$$
$$\varepsilon_i=\frac{LU\mu_2}{\gamma_i\tau},\quad N_{gi}=\frac{L\tau g_x\Delta\rho_{i2}}{\gamma_i},\quad \tau=\sqrt{\kappa},$$
$$M_i=\frac{\mu_i}{\mu_2},\quad X=\frac{x}{L}$$

The system (12) describing steady-state, three-phase flow in heterogeneous medium consists of 2 ordinary differential equations with 6 dimensionless parameters: 2 capillary numbers, 2 gravity numbers and 2 viscosity ratios. The system is coupled even in the case when all the three relative permeabilities are functions of they own saturations only. It consists of two independent equations if :

- one of the phases is immobile, i.e. its individual phase rate is zero,
- relative permeabilities of the other two phases only depend on their own saturation,
- capillary pressure between the mobile phases and the immobile phase only depend on the mobile phase saturation.

Three-phase flow with one phase immobile. Consider a case when the first phase (water) is immobile, i.e. $F_1^0=0$.
If the relative permeability to water is non-zero the equations for the two saturations follow directly from the general case Eq. (12).
If the relative permeability is zero,

$$\lambda_1=0 \qquad (13)$$

the capillarity matrix A degenerates so that the inversion of the matrix may not be performed. For this special case the system (4) becomes

$$U(F_1(S)-F_1^0)=0$$
$$U(F_3(S)-F_3^0)=\kappa(x)\frac{\lambda_2\lambda_3}{\lambda_t}\frac{d\pi_3}{dx} \qquad (14)$$

The first equation of the system (14) is automatically satisfied if the condition (13) is fulfilled. The second equation of the (14) is equivalent to the second equation in the system (8) plus an additional condition requiring that the mobility of the first phase is zero. To demonstrate this we subtract the two equations:

$$(F_3(S)-F_3^0)\frac{\lambda_t}{\lambda_2\lambda_3}-\left[\frac{F_2^0}{\lambda_2}-\frac{F_3^0}{\lambda_3}+\frac{\kappa}{U}g_x\Delta\rho_{32}\right]_{F_1^0=\lambda_1=0}=$$
$$=\frac{1}{\lambda_2\lambda_3}\left[F_3(\lambda_2+\lambda_3)-\lambda_3-\frac{\kappa}{U}g_x\lambda_2\lambda_3\Delta\rho_{32}\right]=$$
$$=\frac{1}{\lambda_2\lambda_3}\left[F_3\lambda_2-F_2\lambda_3-\frac{\kappa}{U}g_x\lambda_2\lambda_3\Delta\rho_{32}\right]=0$$

Similar to the above consideration can be performed for all three phases. This consideration shows that the special case can be obtained as a limiting case of the general system as the phase mobility tends to zero. This observation is important from the point of view of numerical solution of the system of equation, it makes special consideration of the regions with zero phase mobilities unnecessary.

Three-phase flow with one phase mobile. If only water is mobile, i.e. $F_1^0=1$, from the Equation (8) it follows

$$\frac{d\pi_1}{dx}=\frac{U}{\kappa}\left[\frac{1}{\lambda_1}-\frac{\kappa}{U}g_x\Delta\rho_{12}\right]$$
$$\frac{d\pi_3}{dx}=g_x\Delta\rho_{32} \qquad (15)$$

or in case of absence of gravity

$$\frac{d\pi_1}{dx}=\frac{U}{\kappa}\frac{1}{\lambda_1},\quad \frac{d\pi_3}{dx}=0 \qquad (16)$$

If the capillary pressure and the relative permeability to water are only functions of water saturation, then the first equation of the system is exactly the same as in a two-phase case. This means that for the same boundary conditions water saturation does not change with the appearance of gas (e.g. in case of depressurization or gas injection), i.e. some oil will be displaced. The gas-oil capillary pressure will be constant which implies constant gas saturation in a homogeneous reservoir. The value of this constant is defined by the boundary conditions.

Examples.

The question of boundary condition is not trivial. To illustrate the influence of boundary conditions consider numerical examples where the saturation profiles are generated by solving Eq. (12) numerically. Two types of boundary conditions are considered: (1) capillary pressures set to zero at the outlet end which is relevant to laboratory experiments (the so-called outlet end effect), and (2) periodic boundary conditions [3], i.e. $S(0)=S(L)$, which represent infinite porous medium and are relevant for three phase flow in a reservoir away from the wells.

The considered cases correspond to injection of only one phase, water or gas, so that the two others are immobile (capillary trapped). To simplify numerical solution we nevertheless assume all the phases flowing, the fractional flows of the immobile phases are assigned a small value $F_i^0=0.0001$.

The reservoir and fluid parameters used are the following: $L=100cm$, $U=0.0001cm/sec$, $\mu_1=\mu_2=1cps$, $\mu_3=0.02cps$, $k_{ri}=S_i^2$, $I=1,2,3$.

The absolute permeability is presented in Fig. 1. Two different types of oil-water capillary pressure curves is considered, see Fig. 2, which are referred to as mixed-wet and water wet cases. The relative permeabilities and gas-oil capillary pressure (Fig. 3) were the same for all cases. (The capillary pressure curves presented in the figures correspond to the average absolute permeability 1D. They are rescaled to obtain the dimensionless Leverett functions taking into account the heterogeneity, Eq. (11)).

The results of the calculations are shown in Fig. 4 through Fig. 11. For the cases with lab boundary condition (Fig. 4, Fig. 5, Fig. 8, Fig. 9) the saturation of the immobile phase (water or gas) is a constant due to the fact that the zero capillary pressure which is fixed at the outlet boundary remains zero throughout the reservoir. The strong influence of the outlet boundary conditions is therefore observed in both mixed-wet and water-wet lab cases.

This is in contrast with periodic boundary conditions (Fig. 6, Fig. 7, Fig. 10, Fig. 11) for which cases the saturation of neither of the phases is constant. The explanation is straightforward: though the value of the capillary pressure value of the immobile phase is constant the capillary pressure function varies due to heterogeneity and so does the saturation.

The resulting capillary trapped oil saturation for different cases shown in Tables 1 and 2 appears to be different for laboratory and reservoir conditions. The biggest difference is observed in the cases of gas injection and mixed wet rock.

A series of calculations was performed to simulate laboratory experiments performed at high total rate. The total rate was increased 100 times up to 0.01 cm/sec. The resulting immobile oil saturation is shown in Table 3. Though at high rate laboratory experiments the influence of the end effect is minimized the capillary trapping phenomena occurring at reservoir conditions are not correctly captured due to an exaggerated viscous dominance.

Conclusions

The main contribution of this paper is the developed three-phase steady-state model facilitating a rapid simulation of multiphase flow in 1D. The presented numerical examples show that the problem of accurate estimation of capillary trapping from laboratory experiments with heterogeneous cores is difficult to solve even if the cores are relatively long. At low rates which are comparable to the reservoir ones the results are very much influenced by the end effect. At high rates which allow to minimize the end effect the capillary trapping is also minimised due to the viscous dominance which is not relevant at reservoir conditions. The only reasonable way to overcome the difficulties seems to perform the laboratory experiments on homogeneous cores. The problem of heterogeneity should be addressed separately. If the properties of rocks are specified the capillary trapping may be easily calculated using the model described above.

Nomenclature

A = capillarity matrix
F = fractional flow vector function
F^O = fractional flow, a constant vector defined in Eq. (4)
g = acceleration of gravity
J = Leverett J-function
k_r = relative permeability
L = characteristic length
M = viscosity ratio
N_g = gravity number
p = pressure
S = saturation
t = time
u = individual phase velocity
U = total Darcy velocity
x = coordinate
X = dimensionless coordinate
Δ = increment
Δ_s = admissible saturation region defined in Eq. (5)
ε = capillary number
ϕ = porosity
κ = absolute permeability
λ = mobility
μ = viscosity
π = capillary pressure
ρ = density
σ = interfacial tension

Acknowledgment

The work is fulfilled within *RESERVE*, the Norwegian research program. The financial support from the Research Council of Norway and Norsk Hydro a.s. is gratefully acknowledged.

References

1. Aziz, Kh., Settary, A.: *Petroleum reservoir simulation.* Applied science publishers, London. pp. 29-38.
2. Brown, M.: *Differential equations and their applications.* Springer Verlag, New York (1982).
3. Dale, M., Ekrann, S., Mykkeltveit, J., Virnovsky, G. "Effective relative permeabilities and capillary pressure for 1D heterogeneous media." Presented at the 4th European Conference on the Mathematics of Oil Recovery. Røros, Norway 1994.
4. Oak, M.J.: "Three-Phase Relative Permeabilities of Water-Wet Berea," proceedings of the SPE/DOE Symposium on Enhanced Oil Recovery, Tulsa, USA, 1990.
5. Richardson, J.G., Kerver, J.A., Hafford, J.A., and Osoba, J.S.: "Laboratory Determination of Relative Permeability", Trans. AIME, **195** (1952) 187-196.
6. Van Duijn C.J., Molenaar, J., de Neef, M.J. "The effect of capillary forces on immiscible two-phase flow in heterogeneous porous media." *Transport in porous media* **21**, p. 71-93 1995
7. Virnovsky G.A., Helset H.M. and Skjæveland S.M.: "Stability of displacement fronts in WAG operations." SPE 28662. Proc. of the SPE Annual Technical Conference, New Orleans, USA, 1994.
8. Yortsos Y.C., Chang J. "Capillary effects in steady-state flow in heterogeneous cores." *Transport in porous media* **5**. p. 399-420, 1990

Table 1 - Sor at lab boundary conditions

	Water Wet rock	Mixed wet rock
Gas injection	**0.01**	**0.37**
Water injection	**0.02**	**0.14**

Table 2 - Sor at reservoir boundary conditions

	Water Wet rock	Mixed wet rock
Gas injection	**0.21**	**0.05**
Water injection	**0.01**	**0.01**

Table 3 - Sor at lab boundary conditions, high total rate

	Water Wet rock	Mixed wet rock
Gas injection	**0.08**	**0.10**
Water injection	**0.02**	**0.01**

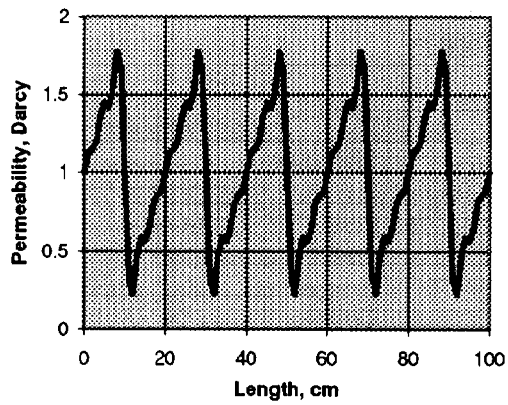

Fig. 1. Absolute permeability

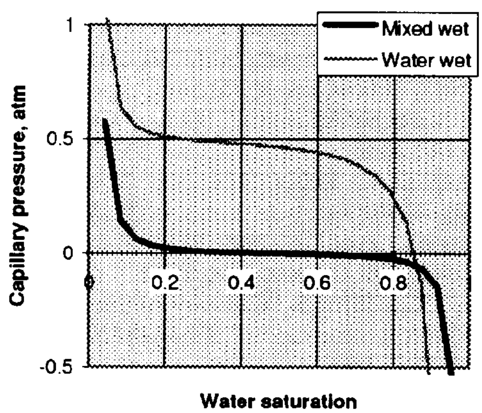

Fig. 2. Oil water capillary pressures corresponding to the absolute permeability 1 D.

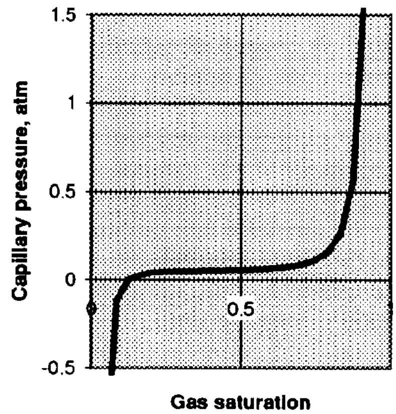

Fig. 3. Gas - oil capillary pressure corresponding to the absolute permeability 1 D.

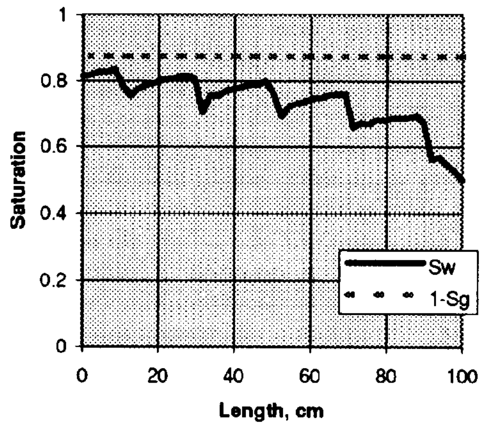

Fig. 4. Water injection at zero capillary pressure at the outlet end, mixed-wet rock

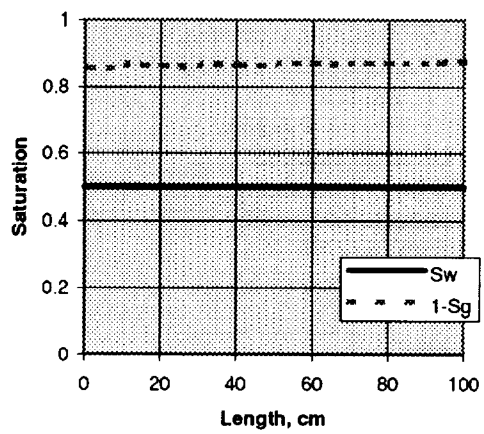

Fig. 5. Gas injection at zero capillary pressure at the outlet end, mixed-wet rock

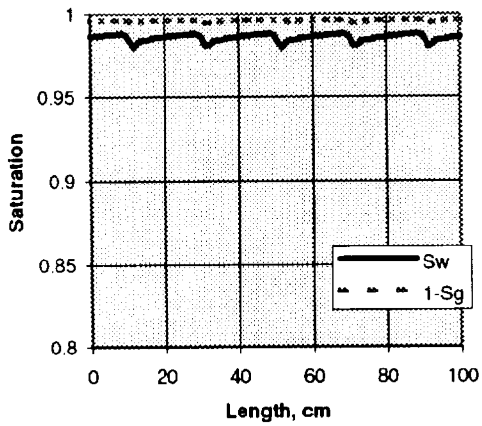

Fig. 6. Water injection at periodic boundary conditions, mixed-wet rock

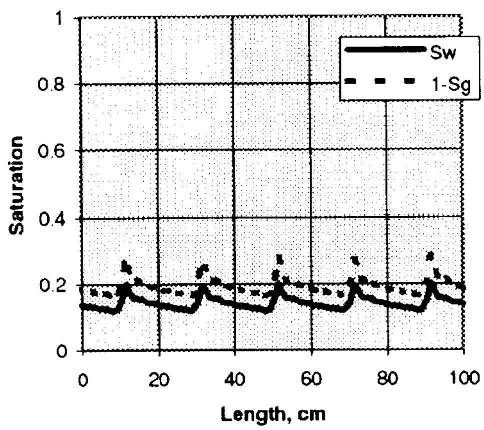

Fig. 7 Gas injection at periodic boundary conditions, mixed-wet rock

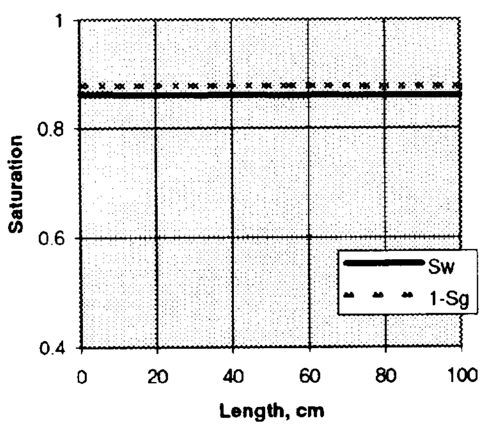

Fig. 8. Water injection at zero capillary pressure at the outlet end, water wet rock

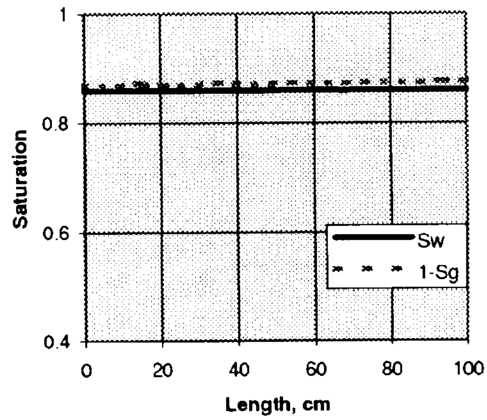

Fig. 9. Gas injection at zero capillary pressure at the outlet end, water wet rock

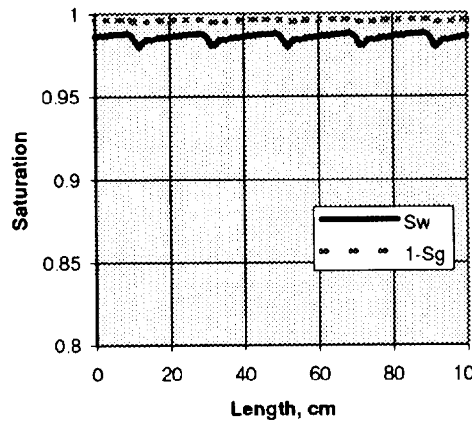

Fig. 10. Water injection at periodic boundary conditions, water wet rock

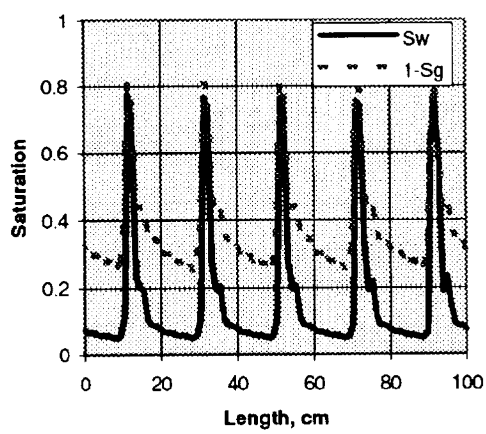

Fig. 11. Gas injection at periodic boundary conditions, water wet rock